Osteoarthritis and Cartilage 27 (2019) 1094–1105

Osteoarthritis and Cartilage

OARSI OSTEOARTHRITIS RESEARCH SOCIETY INTERNATIONAL

CD146/MCAM distinguishes stem cell subpopulations with distinct migration and regenerative potential in degenerative intervertebral discs

S. Wangler † ‡, U. Menzel †, Z. Li †, J. Ma †, S. Hoppe §, L.M. Benneker §, M. Alini †, S. Grad †, M. Peroglio † *

† *AO Research Institute Davos, Switzerland*
‡ *Graduate School for Cellular and Biomedical Sciences, University of Bern, Switzerland*
§ *Inselspital, University of Bern, Switzerland*

ARTICLE INFO

Article history:
Received 14 August 2018
Accepted 3 April 2019

Keywords:
Mesenchymal stem cell
Migration
CD146
Intervertebral disc
Degeneration

SUMMARY

Objective: This study aimed to characterize the mesenchymal stem cell (MSC) subpopulation migrating towards a degenerated intervertebral disc (IVD) and to assess its regenerative potential.
Design: Based on initial screening for migration towards C-C motif chemokine ligand 5 (CCL5), the migration potential of CD146+ and CD146- mesenchymal stem cells (MSCs) was evaluated *in vitro* and in a degenerated organ culture model (degeneration by high-frequency loading in a bioreactor). Discogenic differentiation potential of CD146+ and CD146- MSCs was investigated by *in vitro* pellet culture assay with supplementation of growth and differentiation factor-6 (GDF6). Furthermore, trypsin degenerated IVDs were treated by either homing or injection of CD146+ or CD146- MSCs and glycosaminoglycan synthesis was evaluated by Sulphur 35 incorporation after 35 days of culture.
Results: Surface expression of CD146 led to a higher number of migrated MSCs both *in vitro* and in organ culture. CD146+ and CD146- pellets responded with a similar up-regulation of anabolic markers. A higher production of sulfated glycosaminoglycans (sGAG)/DNA was observed for CD146+ pellets, while in organ cultures, sGAG synthesis rate was higher for IVDs treated with CD146- MSCs by either homing or injection.
Conclusions: The CD146+ MSC subpopulation held greater migration potential towards degenerative IVDs, while the CD146- cells induced a stronger regenerative response in the resident IVD cells. These findings were independent of the application route (injection vs migration). From a translational point of view, our data suggests that CD146+ MSCs may be suitable for re-population, while CD146- MSCs may represent the primary choice for stimulation of endogenous IVD cells.

Introduction

The intervertebral disc (IVD), the largest avascular tissue in the human body, is composed of three main tissues: the annulus fibrosus (AF), the nucleus pulposus (NP) and the cartilaginous endplate (CEP). While the proteoglycan-rich NP binds large amounts of water, the AF and CEP build an envelope containing the NP. This unique architecture allows the IVD to sustain high axial load while providing a wide range of motion[1].

Disc degeneration can be triggered by systemic and environmental factors, such as inadequate load, trauma, smoking, and genetic predisposition[2]. IVD degeneration is a complex, long-lasting process and involves NP fibrosis, AF lamellar organizational changes, and cell activity decrease[3]. Upon degeneration, the disc can no longer sustain the applied mechanical forces, resulting in disc height loss and tissue herniation. Current treatments range from conservative management to surgical intervention. Discectomies and spinal fusions aim to reduce pain and gain stability;

* Address correspondence and reprint requests to: M. Peroglio, AO Research Institute Davos, Clavadelerstrasse 8, 7270, Davos Platz, Switzerland. Tel: +41 081 414 23 91.
E-mail addresses: Sebastian.Wangler@aofoundation.org (S. Wangler), Ursula.Menzel@aofoundation.org (U. Menzel), Zhen.Li@aofoundation.org (Z. Li), Junxuan.Ma@aofoundation.org (J. Ma), Sven.Hoppe@insel.ch (S. Hoppe), LorinMichael.Benneker@insel.ch (L.M. Benneker), Mauro.Alini@aofoundation.org (M. Alini), Sibylle.Grad@aofoundation.org (S. Grad), Marianna.Peroglio@aofoundation.org (M. Peroglio).

https://doi.org/10.1016/j.joca.2019.04.002
1063-4584/

however, no existing clinical treatment induces IVD regeneration. The IVD's avascularity limits the nutrients and oxygen available, resulting in low regenerative capacity[4].

Human mesenchymal stem cells (MSCs) hold promise for biological regeneration of IVDs. *In vitro*, MSCs can differentiate towards an NP-like phenotype under low oxygen culture conditions, hydrostatic pressure or with growth and differentiation factor-5/6 (GDF5, GDF6)[5–7]. Co-cultures with cells isolated from disc tissues induced an up-regulation of IVD markers in MSCs and triggered proliferation and synthesis of extracellular matrix (ECM) by disc cells[8–11]. Multiple *in vivo* studies described a regenerative response in degenerated IVDs following MSC injection[12]. The clinical trials outcomes are mixed: some reported increased disc hydration and pain reduction; others observed no changes after cell treatment[13]. A potential limitation of cell injection is the harsh environment inside degenerated IVDs, especially the low pH which can negatively affect MSC survival[14]. Additionally, the ideal MSC number remains unclear: while clinical trials used up to 31×10^6 MSCs/disc, *in vivo* studies suggest that lower cell numbers hold a higher regenerative effect[15]. Moreover, *in vivo* studies described a needle size/disc height ratio-dependent degenerative response upon AF damage by needle puncture[16].

MSC homing through the CEP may present an alternative MSC delivery route into degenerated IVDs[17]. This concept is based on the natural healing process of MSC-induced regeneration, whereby MSCs migrate towards chemokines released by degenerated disc cells. Following migration, MSCs can induce remodeling of the damaged ECM[18]. However, only few MSCs migrate into the IVD[17]. Identifying the migrating subpopulation would improve the understanding of the migration process and enable the development of regenerative therapies based on selective MSC subpopulations.

In the present work, we identified cluster of differentiation 146 (CD146, also known as melanoma cell adhesion molecule MCAM) as a surface marker to distinguish MSC subpopulations with distinct migration potential toward degenerated IVDs, and assessed CD146+ and CD146- MSCs' direct (differentiation) and indirect (paracrine stimulation) regenerative potential.

Materials and methods

Human mesenchymal stem cell isolation and expansion

Human vertebral bone marrow aspirates were obtained with written consent from patients undergoing spine surgery. MSCs, isolated by Ficoll® gradient centrifugation and adherence to tissue culture plastic, were expanded in alpha-minimum essential medium (αMEM, Gibco, Invitrogen) containing 100 U/mL penicillin, 100 mg/mL streptomycin, 10% fetal bovine serum (FBS, Pan Biotech) and 5 ng/mL basic fibroblast growth factor (Peprotech, Rocky Hill, CT, USA). Early passage (P1–P2) human MSCs from 19 donors were used (Suppl. Fig. 1).

Bovine intervertebral disc isolation

IVDs were harvested from young (n = 24, 6–8 months old) bovine tails obtained from the local abattoir, excised with a band

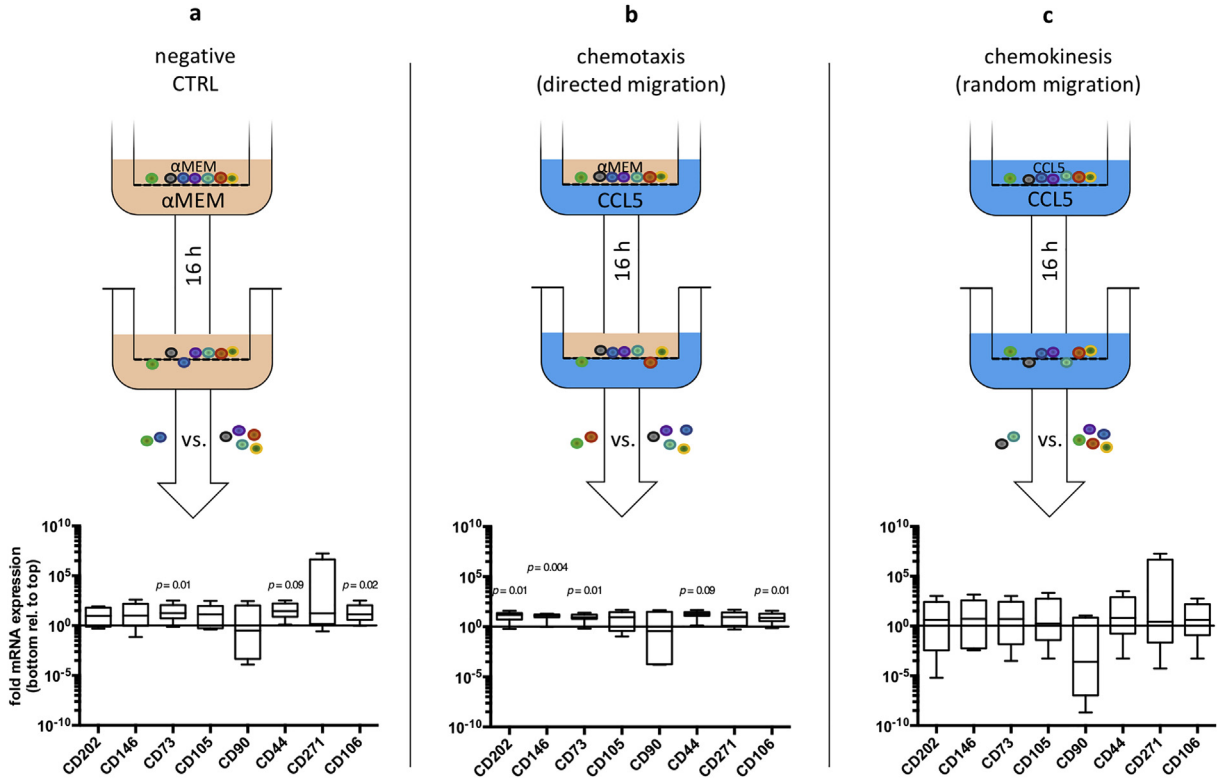

Fig. 1. Scheme representing the *in vitro* trans-well migration assay consisting of a top and bottom chamber, separated by an 8 μm porous membrane, used to isolate the migrating sub-population (bottom chamber) from the non-migrating one (top chamber). Unsorted mesenchymal stem cells (MSCs) were seeded in the top chamber; after 16 h, cells were collected, and RT-PCR was performed. Results are displayed as fold mRNA expression of the migrated subpopulation relative to the cells retained in the top chamber (non-migrated MSCs) (n = 6, age 53 ± 18.2 y). **a)** Negative CTRL, containing αMEM (red) in both the top and bottom chamber. Statistically significant higher expression of CD37, CD44, CD106 was observed in the migrated subpopulation. **b)** Chemotaxis, containing αMEM in the top and CCL5 (100 ng/mL, blue) in the bottom chamber. Statistically significant higher expression of CD202, CD146, CD73, CD44 and CD106 was found in the migrated subpopulation. **c)** Chemokinesis, containing CCL5 (100 ng/mL) in both chambers. No significant changes in the gene expression profile in the migrating sub-population were observed.

Table I
List of human genes analyzed by real-time RT-PCR in the migration experiments

	Gene	Name	Function	Assay ID
CD73	NT5E	5′-nucleotidase	Converts AMP to adenosine	Hs00159686_m1
CD90	Thy-1	glycophosphatidylinositol	Cell-cell and cell-matrix interactions	Hs00264235_s1
CD105	ENG	endoglin	Part of TGFb receptor complex	Hs00923996_m1
CD202	Tie2	angiopoietin receptor	Receptor for Ang1/4	Hs00176096_m1
CD271	LNGFR	low-affinity nerve growth factor receptor	TNF receptor	Hs00609977_m1
CD44	HCAM	homing cell adhesion molecule	Cell adhesion and migration	Hs01075861_m1
CD146	MCAM	melanoma cell adhesion molecule	Cell adhesion molecule	Hs00174838_m1
CD106	VCAM-1	vascular cell adhesion molecule 1	Cell adhesion molecule	Hs01003372_m1
18S	–	18S ribosomal RNA	Endogenous control	Hs 99999901_s1

saw (Exakt Apparatebau), rinsed in phosphate buffered saline (PBS) containing 10% penicillin-streptomycin[19] and cultured in:

1. **LG-DMEM**: Dulbecco's Modified Eagle Medium (DMEM) containing 1 g/L glucose, 25 mM Hepes (Gipco, cat. *n*. 15,630–056), 2% fetal bovine serum (FBS), 100 U/mL penicillin, 100 μg/mL streptomycin, 1% insulin-transferrin-selenium (ITS+, Corning, cat. *n*. 354352), 50 μg/mL Primocin (for high-frequency loading-induced IVD degeneration);
2. **HG-DMEM**: DMEM containing 4.5 g/L glucose, 2 mM Glutamax, 25 mM Hepes, 5% FBS, 100 U/mL penicillin, 100 μg/mL streptomycin, 50 μg/mL L-ascorbate, 50 μg/mL Primocin (for trypsin-induced IVD degeneration).

Induction of intervertebral disc degeneration

Bovine IVDs were punched (22G needle) and cultured in LG-DMEM in a bioreactor system under degenerative high-frequency loading (0.6 ± 0.2 MPa; 10 Hz, 4 h/day) for 7 days[17]. Medium was changed daily, pooled and collected as disc conditioned medium (CM).

Gene-expression profile of MSCs migrated towards CCL5

A 6-well trans-well system consisting of top and bottom chambers separated by an 8 μm porous membrane was used for the migration assay (Costar, cat. *n*. 3428). Chambers were filled with αMEM and pre-incubated at 37°C for 2 h. Following standard migration protocols, MSCs (n = 6, age 53 ± 18.2 y) were serum-starved for 6 h prior to seeding (top chamber, αMEM, 3×10^5 cells/well)[20]. C-C motif chemokine ligand 5 (CCL5), a key chemokine released by degenerative IVDs, was used as chemo-attractant[21] in the bottom chamber at 100 ng/mL (chemotaxis group, Fig. 1b)[22]. Controls included random migration in CCL5 (= chemokinesis; CCL5 in top and bottom chamber, Fig. 1c) and migration without CCL5 (= CTRL; αMEM in top and bottom chamber, Fig. 1a). After 16 h, migrated and non-migrated cells were collected separately by trypsinization, washed in PBS, lysed with 0.5 mL TRI-reagent and 2.5 μL polyacryl carrier (Molecular Research Center, Cincinnati) and reverse-transcribed with SuperScript Vilo cDNA Synthesis kit (Invitrogen, Thermo Fisher Scientific). Expression levels of genes of interest (Table I) were measured by real-time PCR (QuantStudio six Flex: Applied Biosystems) using Gene expression assays (Thermo Fisher Scientific). For relative quantification, the dCt method was used with 18s rRNA as endogenous control. Genes were selected based on surface markers involved in MSC homing, i.e., MSC markers found on degenerated IVD cells (CD73, CD90, CD105)[23], NP-cell progenitor markers (CD202, CD271)[24] and MSC migration-associated markers (CD44, CD146, CD106)[25–27].

CD146 expression of MSCs exposed to intervertebral disc conditioned medium

MSCs (n = 5, age 58 ± 12.7 y) were seeded (6×10^4 cells/cm^2) in a 6-well plate containing either 2 mL LG-DMEM or CM (Fig. 2a). After 16 h, cells were trypsinized, and CD146 expression (PECy7 1:20, BD cat. *n*. 562135) was analyzed by flow cytometry (BD FACSAria III).

Migration potential of CD146+ and CD146- MSCs in vitro

The trans-well migration was repeated using CM (Fig. 2c). MSCs (n = 6, age 44 ± 21.9 y), separated in CD146+ and CD146- populations through fluorescence-activated cell sorting (FACS, Fig. 3c) using the PECy7 antibody (BD cat. *n*. 562135, 1:20), were plated in LG-DMEM in the top chamber (3×10^5 cells/well). Purity range after sorting was >97% and >98% for CD146+ and CD146- MSCs, respectively. After 16 h, migrated and non-migrated cells were collected as described above and counted (Scepter™ 2.0 Cell Counter, Merck Millipore).

Homing of CD146+ and CD146- MSCs into whole intervertebral discs

MSCs (n = 3, age 41.6 ± 30.7 y), separated in CD146+ and CD146- subpopulations by FACS, were stained with a fluorescent membrane dye (PKH Fluorescent Cell Linker Kit; Sigma–Aldrich) according to manufacturer's instructions (CD146+ and CD146- MSCs were labeled with PKH26 (red), and PKH67 (green) respectively). Each MSC subpopulation was placed on a separate, randomly selected, degenerative IVD (Fig. 3a). A 30 μL suspension (containing 1×10^6 MSCs in LG-DMEM) was added on the IVD endplate (Fig. 3b)[17]. After 20 min, IVDs were covered with LG-DMEM and cultured in free-swelling conditions with medium change every 48 h. After 5 days of migration, IVDs were sagittally-cut with a Padgett blade using a custom-made holding device and visualized on a motorized microscope (Axiovert 200 m, Zeiss) in epifluorescence at 2.5× magnification. MSC engraftment was analyzed by measuring the IVD area and manually counting the migrated fluorescent-labelled cells.

Discogenic in vitro pellet differentiation of CD146+ and CD146- MSCs

The differentiation potential towards a discogenic phenotype was investigated using a pellet-culture model[28]. Briefly, MSCs (n = 4, age 61.4 ± 7.1y) were separated in CD146+ and CD146- subpopulations by FACS and dispensed into 15 mL tubes (2.5×10^5 cells) in 2 mL of 4.5 g/L glucose Dulbecco's Modified Eagle Medium (DMEM) containing 1% FBS, 1% ITS+, 100 U/mL penicillin,

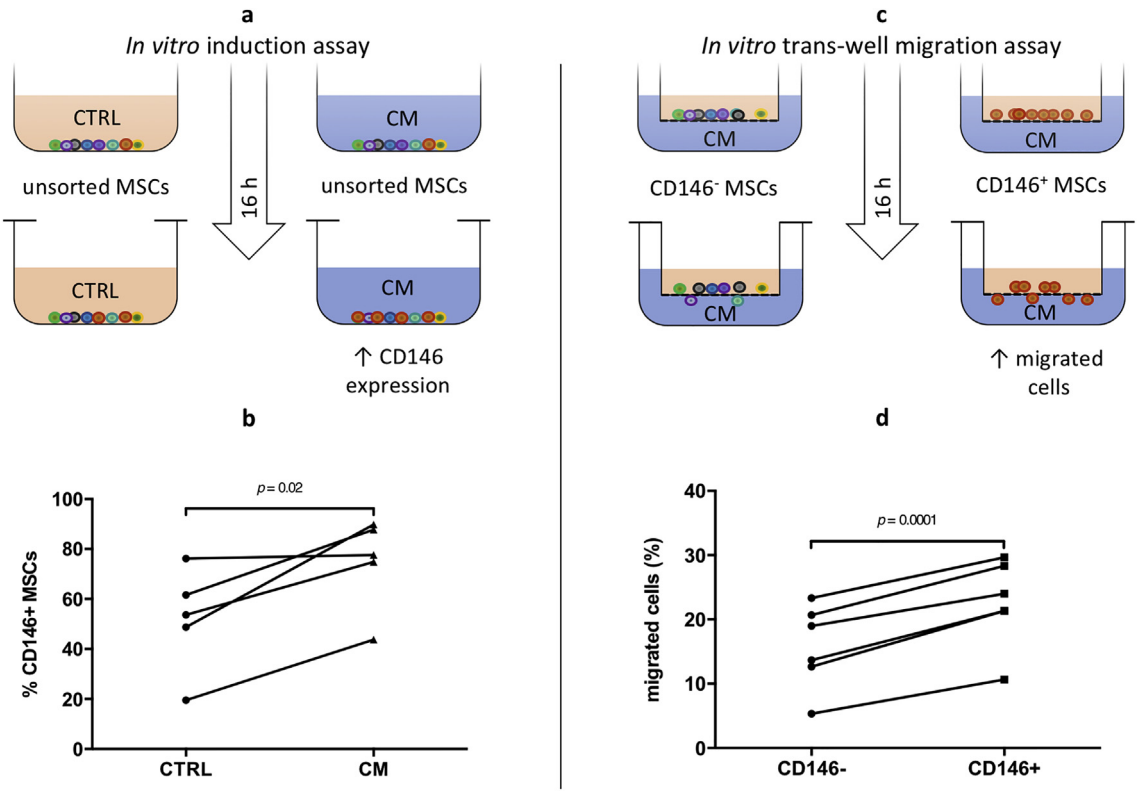

Fig. 2. a) Scheme representing the *in vitro* induction assay. Unsorted MSCs were either exposed for 16 h to LG-DMEM (CTRL) or conditioned medium (CM) and protein expression of CD146 was measured by flow cytometry. **b)** Exposure of unsorted MSCs to CM induced a significant upregulation of CD146 protein expression ($n = 5$, age 58 ± 12.7 y). **c)** Scheme representing the *in vitro* trans-well migration assay. FACS-sorted CD146 + or CD146- MSCs were seeded in the top chamber and CM was placed in the bottom chamber; after 16 h the number of migrated cells was quantified. **d)** Protein expression of CD146 led to a statistically significant higher fraction of migrating cells ($n = 6$, age 44 ± 21.9 y).

100 μg/mL streptomycin, 100 μM ascorbic acid-2- phosphate, 10^{-7} M dexamethasone, 40 μg/mL L-proline, 100 ng/mL GDF6 (BMP-13, cat. *n*. AF-120-04, PrepoTech). Pellets were cultured for 14 days with medium change every 48 h (Fig. 4a). A sample (2.5×10^5 cells) of the unsorted MSC population was collected at day 0 for reference.

Gene expression by quantitative real-time RT-PCR

After 14 days, pellets were lyzed in 0.5 mL TRI reagent and 2.5 μL polyacryl carrier with a pellet grinder (Sigma–Aldrich, cat. *n*. Z359971). RNA isolation and reverse transcription were performed as described above. Expression levels of genes of interest (Table II) were measured by real-time PCR (QuantStudio six Flex: Applied Biosystems) using the dCt method with 18s rRNA as endogenous control.

Sulphated glycosaminoglycan production

Sulfated glycosaminoglycan (sGAG) production was assessed in triplicate using a dimethylmethylene blue (DMMB, pH = 3) assay and chondroitin sulfate C (shark cartilage, Sigma) as standard. The total DNA content was measured by Hoechst dye assay, according to manufacturer's instructions (Thermofisher, cat. *n*. 33-258). For pellets, sGAG values were normalized to DNA content (μg/μg); sGAG released in the medium during culturing was measured and normalized to pellet DNA content.

ECM deposition by histology and immunohistochemistry

Pellets were washed (PBS), fixed (70% methanol, 4°C, 5 days), rehydrated overnight (5% sucrose in PBS) and embedded in cryocompound; 10 μm sections were cut (Microm HM560) and stained (Safranin O/Fast Green). Immunohistochemistry using antibodies against collagen type I (Col1) and II (Col2) (Col1/CIIC1, Department of Biological Services University of Iowa) was performed[29].

Pellet stiffness and size

Pellets were washed, fixed and rehydrated as described above, and stiffness of fully-hydrated pellets in PBS was determined using the Piuma Nanoindenter (Optics 11) (indentation probe stiffness = 47 N/m, tip radius = 29 μm, Optics 11) at three different points (pellet rotation in-between) with three measurements per point. The Young's modulus was calculated using the Oliver and Pharr's method[30]. Results are represented as the mean of nine measurements/pellet. Pellet diameter was measured from three different angles (random location, 180° flip, 90° flip); the average was used to calculate the volume of a sphere representing the pellet.

Intervertebral disc regeneration using CD146+ and CD146- stem cell subpopulations

Bovine IVDs ($n = 18$ discs, diameter: 17–20 mm; two tails 7 and 8-months old) were enzymatically-treated by a single injection of trypsin dissolved in PBS (750 μg trypsin/disc; 1995 BAEE U/mg,

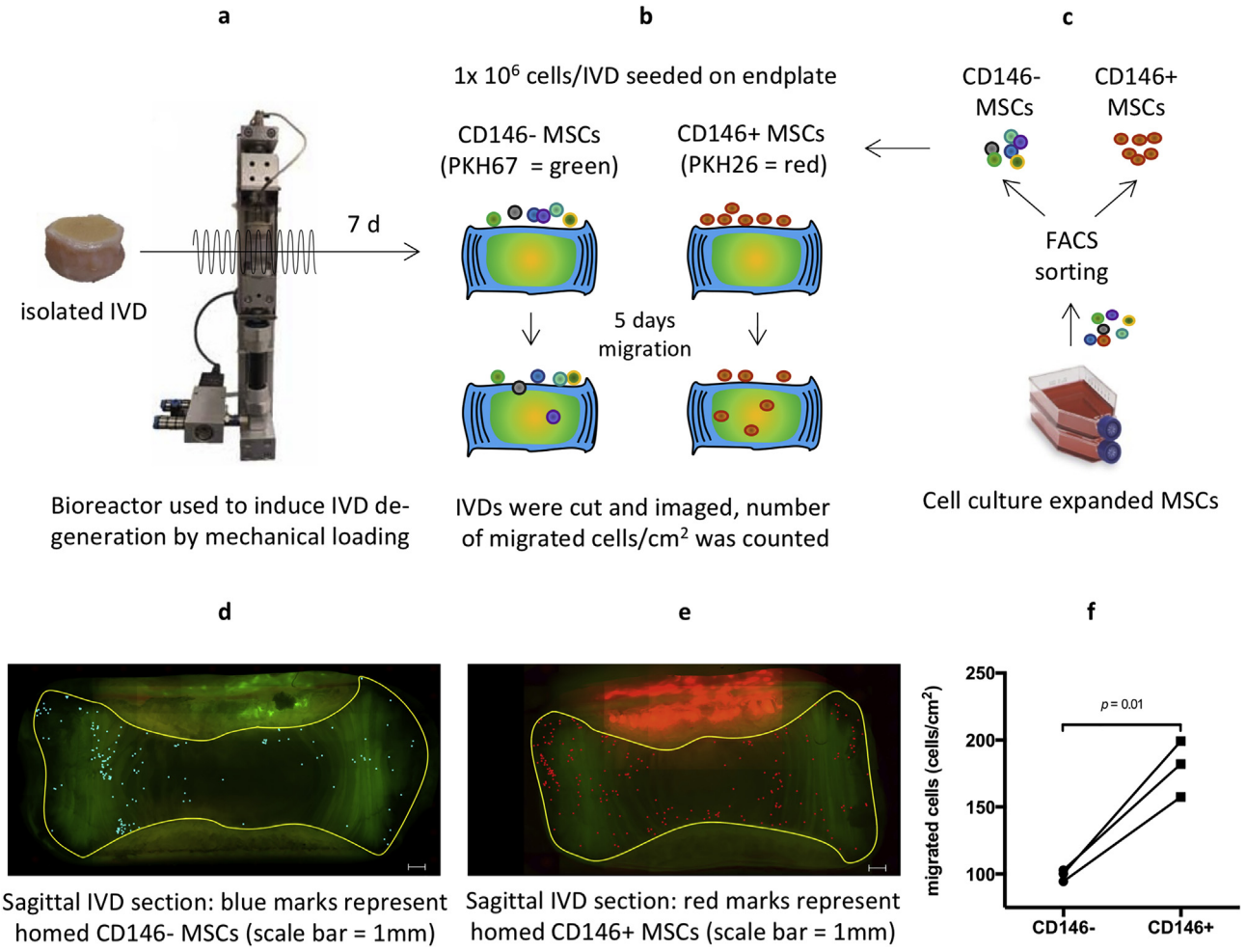

Fig. 3. Scheme representing the organ culture migration assay: **a)** High frequency loading in a bioreactor was used to induce degeneration in the isolated intervertebral disc (IVD) (0.6 MPa ± 0.2; 10 Hz, 7 d, 4 h/day); **b)** PKH-labeled CD146 + and CD146- MSCs were seeded on the endplate of induced degenerated IVDs; after 5 days, discs were fixed and number of migrated MSCs was counted; **c)** Culture-expanded MSCs were sorted into CD146 + and CD146- subpopulations through fluorescence-activated cell sorting. **d)** Fluorescent image of IVD cross-section: CD146- migrated cells were market by blue dots, yellow line indicates contour of the IVD. **e)** Fluorescent image of IVD cross-section: CD146 + migrated cells were market by red dots, yellow line indicates contour of the IVD. **f)** Expression of CD146 resulted in a statistically significant higher number of migrated MSCs towards induced-degenerative disc tissue (179.6 ± 29.6 cells/cm^2) compared to the CD146- MSCs (99.2 ± 4.3 cells/cm^2) (n = 3, age 41.6 ± 30.7 y).

Sigma Aldrich, cat. *n*. T4799-5G) into the NP. Following a 14-day free-swelling culture in HG-DMEM (Fig. 6)[31], FACS-sorted CD146+/CD146- MSCs (n = 3, age 41.6 ± 30.7 y) were either seeded on the endplate (1×10^6 cells/disc, tail 1, Fig. 6a) or injected (1×10^6 cells/disc in 30 μL PBS, tail 2, Fig. 6b) into the NP with a 22G needle. The same MSC donors (ID: 17–19, Suppl. Fig.1) were used for migration and injection experiments; discs were randomly assigned to either treatment by CD146+ or CD146- cells. Each experiment was performed with IVDs from one tail to exclude tail variability. From each tail, an untreated IVD was used as a positive control (ctr) and a trypsin-injected (without MSCs) IVD as a negative control (trypsin). After MSC application, discs (including controls) were kept in culture for 21 days under free-swelling conditions in HG-DMEM, with medium change every 48 h.

Sulphated glycosaminoglycan synthesis activity of stem-cell treated intervertebral discs

Twenty-one days after MSC application (= 35 days total IVD culture), endplates were removed with a scalpel. NP and AF were separated with a biopsy punch; 30–40 mg from each tissue type were placed in a 12-well plate, cultured for 18 h in HG-DMEM containing ^{35}S-sulfate (2.5 μCi/mL), followed by washing in PBS and digestion in 0.5 mL proteinase K solution (Roche, 0.5 mg/mL) at 56°C overnight. Incorporated ^{35}S-sulfate was analyzed using size exclusion PD-10 columns and liquid scintillation counting[17]. Total DNA content of digested tissue (measured by Hoechst dye) was used to normalize GAG synthesis activity.

Histological evaluation

At day 35, positive and negative control discs were sagittally-cut using a Padgett blade with a custom-made holding device. Disc halves were fixed (4% buffered paraformaldehyde, 3 days), and decalcified (ethylenediaminetetraacetic acid, 4 weeks); paraffin sections (5 μm thick) were stained with Safranin-O/Fast Green[32] and immunohistochemical staining for collagen type I (Acris #R1038, 1:400) and collagen type II (CIIC1, 2 μg/mL IgG, Department of Biological Services University of Iowa) was performed after enzymatic pre-treatment (25 mg/mL hyaluronidase, Sigma #H3506 + 0.25 U/mL chondroitinase ABC, Sigma #C2905, at 37°C for 30 min). The antibody incubation was performed overnight at 4°C. After enzymatic pretreatment (as described above), immunohistochemical staining for aggrecan

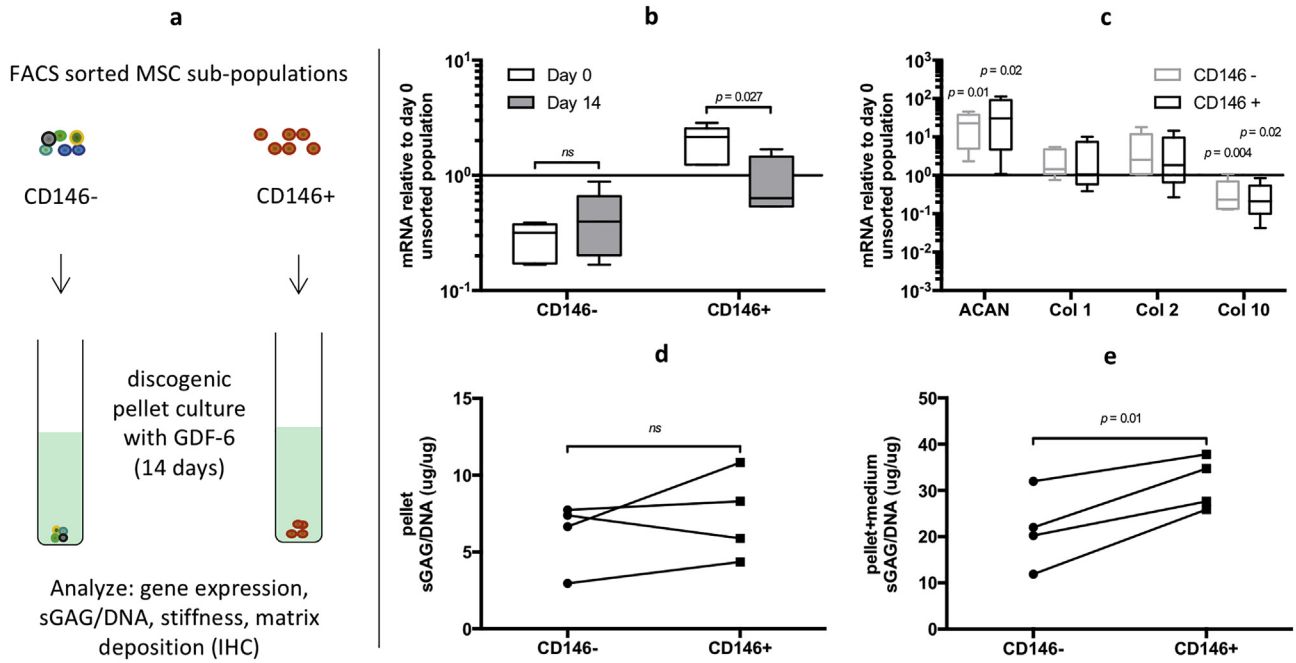

Fig. 4. a) Scheme representing the *in* vitro discogenic pellet culture assay. CD146+ or CD146- MSCs were cultured as pellets in medium containing 100 ng/mL GDF-6; after 14 days the gene expression, sulfated glycosaminoglycan (sGAG) production, pellet stiffness, and matrix deposition were analyzed. The gene expression data represents 2^{-ddCt} relative to the unsorted population at day 0. **b)** CD146 expression was unchanged over time for CD146- pellets, whereas CD146+ pellets responded with a statistically significant down-regulation of CD146 following 14 days of culture. **c)** CD146+ and CD146- pellets responded with a similar and statistically significant up-regulation of ACAN and downregulation of Col 10 compared to day 0 sorted populations. **d)** Deposition of sGAG was measured by DMMB assay and normalized to the pellets DNA content. No difference was found for sGAG in CD146+ vs CD146- pellets. **e)** A statistically significant higher production of total sGAG/DNA (= pellet and medium) was observed for CD146+ pellets ($n = 4$, age 61.4 ± 7.1 y).

(12/21/1-C-6, 4 ug/mL IgG, Developmental Studies Hybridoma Bank, University of Iowa) was performed overnight at 4°C, and followed by reduction and alkylation[33]. This was followed by incubation with a biotinylated secondary antibody (Col2 and aggrecan: horse anti-mouse, Col1: goat anti-rabbit), avidin-biotin-peroxidase (Vectastain Elite ABC kit, Vector Laboratories) and DAB (Vector Laboratories). Negative control sections were incubated without the primary antibody. Sections were imaged in transmitted light using an Axioplan 2 (Zeiss) with a 1.25× objective and a B×63 (Olympus) microscope with a 40× objective.

Statistical analysis

Statistical analyses were conducted in R Studio v1.1.456 (R v3.4.4) with $P \leq 0.05$ considered statistically different. Data distribution was displayed as QQ-Plots and normality checked with the Shapiro–Wilk test. When the normality assumption was satisfied, a paired Student *t*-test was chosen to compare CD146+ and CD146- MSC subpopulations from the same MSC donor. Results of the organ culture regeneration assay (Fig. 6d) were not normally distributed and a paired non-parametric *t*-test was conducted (Wilcoxon matched-pairs signed rank test). Each data point in the figures represents an MSC donor; lines connect same-donor results. Gene expression results are displayed as box plots (Figs. 1 and 4). Error bars of organ culture regeneration assays indicate 95% CI (Fig. 6). Unless indicated otherwise, "$n =$ " refers to the number of MSC donors. For additional clarity, means ± standard deviations are provided in the results section.

Results

CD146/MCAM characterizes an MSC subpopulation with a higher migration potential towards intervertebral discs

To characterize the gene expression profile of the migrating MSC subpopulation, an *in vitro* trans-well assay using CCL5 as chemo-attractant was performed. Overall, migrated MSCs showed an up-

Table II
List of human genes analyzed by real-time RT-PCR in the differentiation experiments

Abb.	Name	forward primer seq	reverse primer seq	Probe seq
ACAN	Aggrecan	5′-AGT CCT CAA GCC TCC TGT ACT CA-3′	5′-CGG GAA GTG GCG GTA ACA-3′	5′-CCG GAA TGG AAA CGT GAA TCA GAA TCA ACT-3′
Col 1	Collagen 1 alpha1	5′-CCC TGG AAA GAA TGG AGA TGA T-3′	5′-ACT GAA ACC TCT GTG TCC CTT CA-3′	5′-CGG GCA ATC CTC GAG CAC CCT -3′
Col 2	Collagen 2 alpha2	5′-GGC AAT AGC AGG TTC ACG TAC A-3′	5′-GAT AAC AGT CTT GCC CCA CTT ACC-3′	5′-CCT GAA GGA TGG CTG CAC GAA ACA TAC-3′
Col 10	Collagen 10	5′-ACG CTG AAC GAT ACC AAA TG-3′	5′-TGC TAT ACC TTT ACT CTT TAT GGT GTA-3′	5′-ACT ACC CAA CAC CAA GAC ACA GTT CTT CAT TCC-3′
RunX2	Runt-related transcription factor 2	5′-AGC AAG GTT CAA CGA TCT GAG AT-3′	5′-TTT GTG AAG ACG GTT ATG GTC AA-3′	5′-TGA AAC TCT TGC CTC GTC CAC TCC G-3′
Sox9	SRY (sex determining region Y)-box 9	Assay ID: Hs00165814_m1		

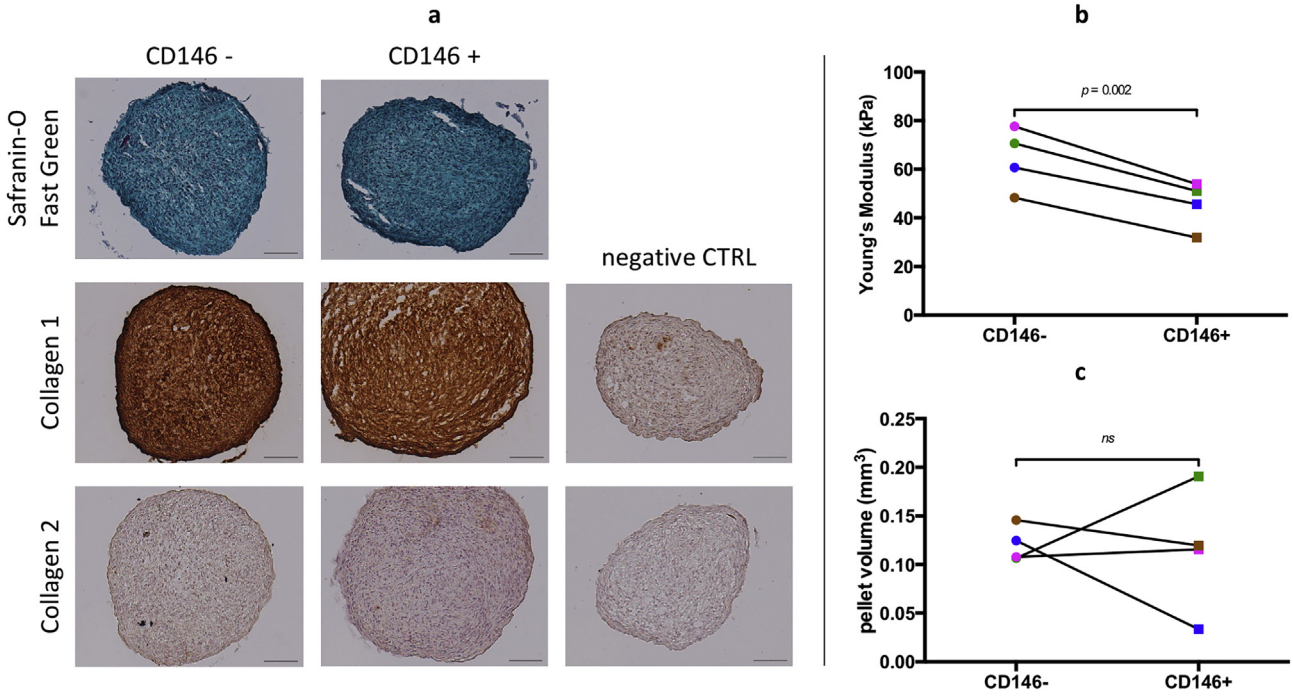

Fig. 5. a) Safranin-O/Fast green, collagen type one and two staining of CD146+ and CD146- pellets (scale bar = 100 μm); collagen type one was prevalent. **5 b/c)** Pellet stiffness assessment by nanoindentation: CD146- pellets had a statistically significant higher stiffness (64.3 ± 12.7 kPa) compared to CD146+ pellets (45.6 ± 9.7 kPa), irrespective of pellet volume. Donors are color-coded to allow comparison ($n = 4$, age 61.4 ± 7.1 y).

regulation of the investigated genes relative to non-migrated cells (Fig. 1a and b, $n = 6$, age 53 ± 18.2 y). A statistically significantly higher mRNA expression (migrated vs non-migrated) was detected in the CTRL and chemotaxis groups for CD44, CD73 and CD106 (Fig. 1a and b). No differences could be observed in the chemokinesis group (Fig. 1c). A significant up-regulation of CD146 (12.7 ± 6.4 fold, $P = 0.004$) and CD202 (15.9 ± 13 fold, $P = 0.013$) was observed solely in the chemotaxis group (Fig. 1b). Thus, these two markers were further assessed at the protein level by flow cytometry on culture-expanded MSCs. Less than 1% of the MSCs expressed CD202, while CD146 was expressed on 60–90% of the MSCs. With clinical translation as the end-goal, we focused on CD146 as a potential predictive marker.

Migrating MSCs are exposed to a complex combination of factors released by the degenerated IVDs[21]. To investigate their effect on CD146 surface protein expression, we exposed MSCs to CM from induced-degenerative IVDs (Fig. 2a). This induced a significant increase in CD146 expression (61.7 ± 18.8%) compared to culture in basal medium (43.5 ± 28%) (Fig. 2b; $P = 0.023$).

To investigate if CD146 identifies an MSC subpopulation with enhanced migration potential, *in vitro* and organ culture migration assays were performed. Using CM as chemoattractant in the transwell assay (Fig. 2c), the proportion of migrating MSCs was higher for CD146+ (22.5 ± 6.8% migrated cells) compared to CD146- (15.7 ± 5.6 % migrated cells) MSCs (Fig. 2d; $P = 0.0001$). Organ cultures confirmed that CD146+ MSCs migrated in higher numbers towards induced-degenerative disc tissue (179.6 ± 29.6 cells/cm^2) compared to CD146- MSCs (99.2 ± 4.3 cells/cm^2) (Fig. 3d–f; $P = 0.016$).

CD146+ MSCs have higher discogenic differentiation potential in vitro

The discogenic differentiation potential of CD146+ vs CD146- MSCs was analyzed following a 14-day pellet culture in GDF6-supplemented medium (Fig. 4a). Gene expression levels at day 14 were normalized to the unsorted MSC population on day 0 to allow for comparison of CD146+ and CD146- MSC subpopulations. Gene expression of CD146 decreased in the CD146+ pellets (2.1 fold; $P = 0.027$) following a 14 day-culture, whereas it did not change significantly (1.5 fold; $P = 0.187$) over time in the CD146- sorted subpopulation (Fig. 4b). CD146+ and CD146- pellets responded with a similar, statistically significant, up-regulation of ACAN (CD146+: 10.07 fold; $P = 0.025$. CD146-: 8.32 fold; $P = 0.014$) and down-regulation of Col 10 compared to the day 0 sorted populations (CD146+: 0.22 fold; $P = 0.027$, CD146-: 0.32 fold $P = 0.004$) (Fig. 4c). Col1 and Col2 expression in the CD146+ and the CD146- pellets did not differ over time (Fig. 4c).

While no difference in sGAG/DNA ratios was found inside CD146+ pellets and CD146- pellets (6.9 ± 3.4 and 5.9 ± 2.7, respectively) (Fig. 4d), a higher production of total sGAG/DNA (= pellet + medium) was observed for CD146+ pellets (28.3 ± 8.6 and 21.3 ± 7.1, respectively) (Fig. 4e; $P = 0.015$). Immunohistochemical staining for Col1 and Col2 showed that CD146+ and CD146- pellets were mostly composed of Col1 with a denser structure in the CD146- pellets (Fig. 5a). The CD146+ pellets, capable of producing more GAG, were also less stiff compared to CD146- pellets (respectively, 45.6 ± 9.7 kPa and 64.3 ± 12.7 kPa), as attested by nanoindentation (Fig. 5b; $P = 0.002$). Pellet size was similar for both groups (Fig. 5c).

CD146- MSCs induce a higher regenerative response in degenerative intervertebral discs

To investigate the regenerative capacity of CD146+ and CD146- MSCs in organ culture, we treated degenerated IVDs with either MSC injection or homing (Fig. 6). For both strategies, the sGAG synthesis rate was higher in CD146- treated IVDs, suggesting that the secretome of this subpopulation might hold a higher

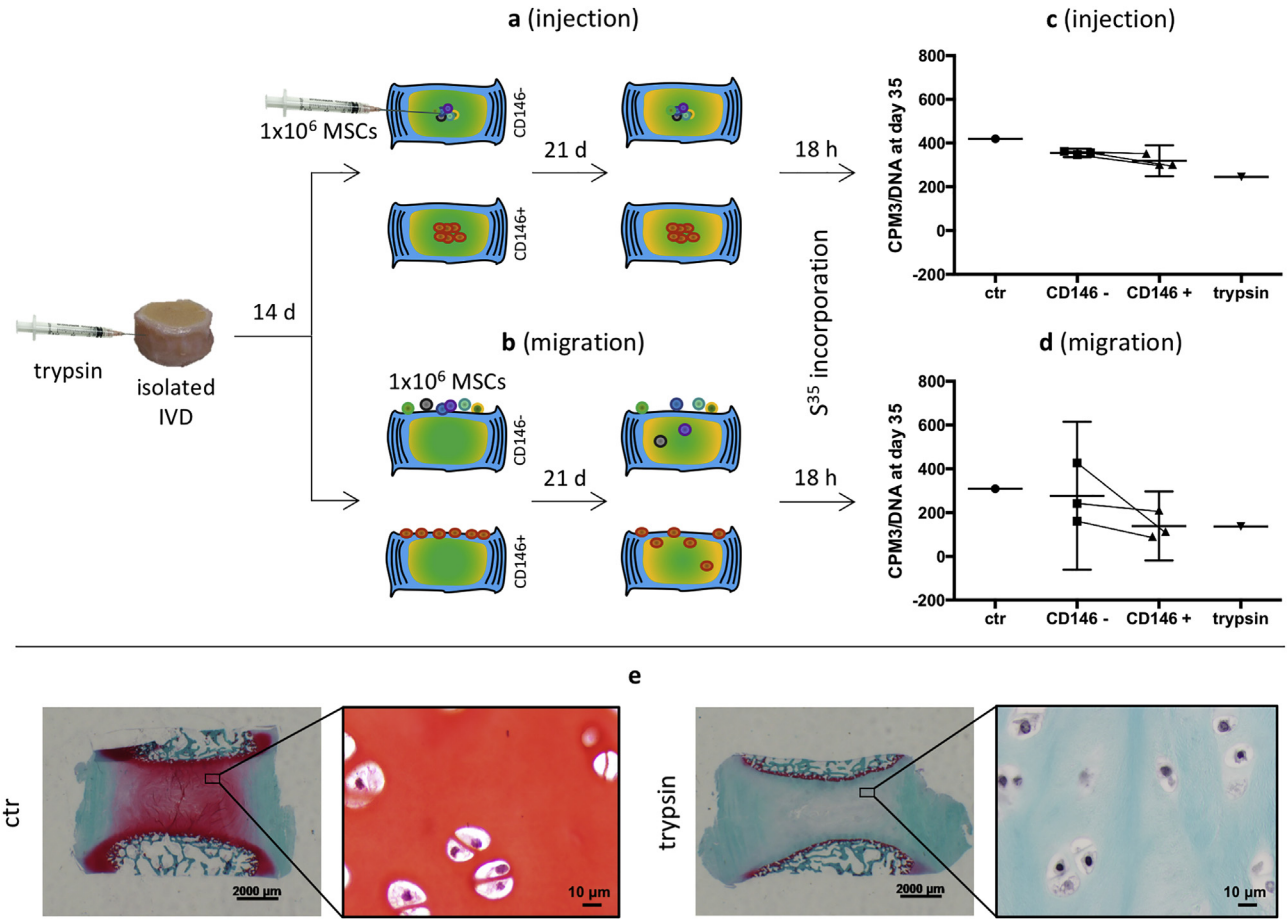

Fig. 6. Scheme representing the trypsin-induced IVD degeneration; 14 days following the trypsin injection, degenerated IVDs were treated by either **a)** injection of MSCs with a 22G needle or **b)** MSC migration. **c/d)** Trypsin-injected IVDs (trypsin) had a lower sGAG synthesis rate than the untreated control (ctr). In both injection and homing groups, all discs had a higher sGAG synthesis rate when treated with CD146- sorted MSCs compared to CD146+ MSCs. **e)** Safranin-O fast green staining of trypsin injected IVDs did not reveal changes of disc cell morphology after 35 days (IVDs $n = 16/2$ tails, MSCs $n = 3$, age 41.6 ± 30.7 y).

regenerative potential. Interestingly, this trend was consistently observed both with CD146- MSC injection and migration (Fig. 6 c,d). From a translational point of view, our data suggest that MSC homing might have a similar stimulatory effect on IVD cells as injection (Suppl. Fig. 2a). Safranin-O/Fast Green staining of trypsin-injected IVDs did not reveal changes of disc cell morphology after 35 days [Fig. 6e].

The major difference between IVDs (Safranin O/Fast green-stained) was observed when comparing discs with and without trypsin injection, independent of MSC type and application mode (Figs. 6e and 7 and Suppl. 3). Indeed, trypsin-injected discs showed a faint Safranin O staining, thus attesting proteoglycan depletion, in agreement with findings by Haglund's group[31]. When comparing CD146+ vs CD146- MSCs, no major differences between treated IVDs were observed (i.e., the original proteoglycan content was not restored). When comparing MSC injection and migration, no major differences were observed between treated IVDs (Fig. 7 and Suppl. Fig. 3). With injected MSCs, cell agglomerates were visible in the center of the IVD, while with migrated MSCs, these cells cannot be distinguished from the IVD cell population (Fig. 8).

Closer examination of immunohistochemical staining of MSC-injected IVDs allowed the evaluation of both MSC differentiation and IVD tissue response (with three MSC donors). Both IVD tissue and MSCs were positive for aggrecan; CD146+ and CD146- MSCs showed a similar staining intensity, but tissues treated with CD146- MSCs always showed a more intense aggrecan staining (Fig. 8 d-f, k-m). Both injected MSCs and IVD tissues were positive for Col1, although the staining was faint in all trypsin-injected IVDs. MSCs agglomerates and surrounding tissue were more intensely stained for CD146- compared to CD146+ MSCs (two out of three donors, Fig. 8 b,e,i,l). CD146+ and CD146- MSCs were negative for Col2, but IVD tissue was more intensely stained when CD146- MSCs were injected (Fig. 8 c,f,j,m).

Discussion

This study investigated the ability of MSC populations to migrate into IVDs and initiate a regenerative reaction. Concerning the MSC source, it has been shown that MSCs from vertebral biopsies exhibited the same phenotype, proliferative and adipogenic potential, but higher osteogenic and chondrogenic differentiation capabilities than MSCs from the iliac crest[34]. Only bone marrow biopsies from vertebral bodies were included in this study because vertebral bone marrow MSCs would naturally be recruited towards a degenerative disc in a physiological setting[17]. As MSCs lose the differentiation and migration potential with increasing passage number, only early passage (P1–P2) human MSCs were included[17,35]. Moreover, early passage MSCs are generally used in clinical trials[36–38].

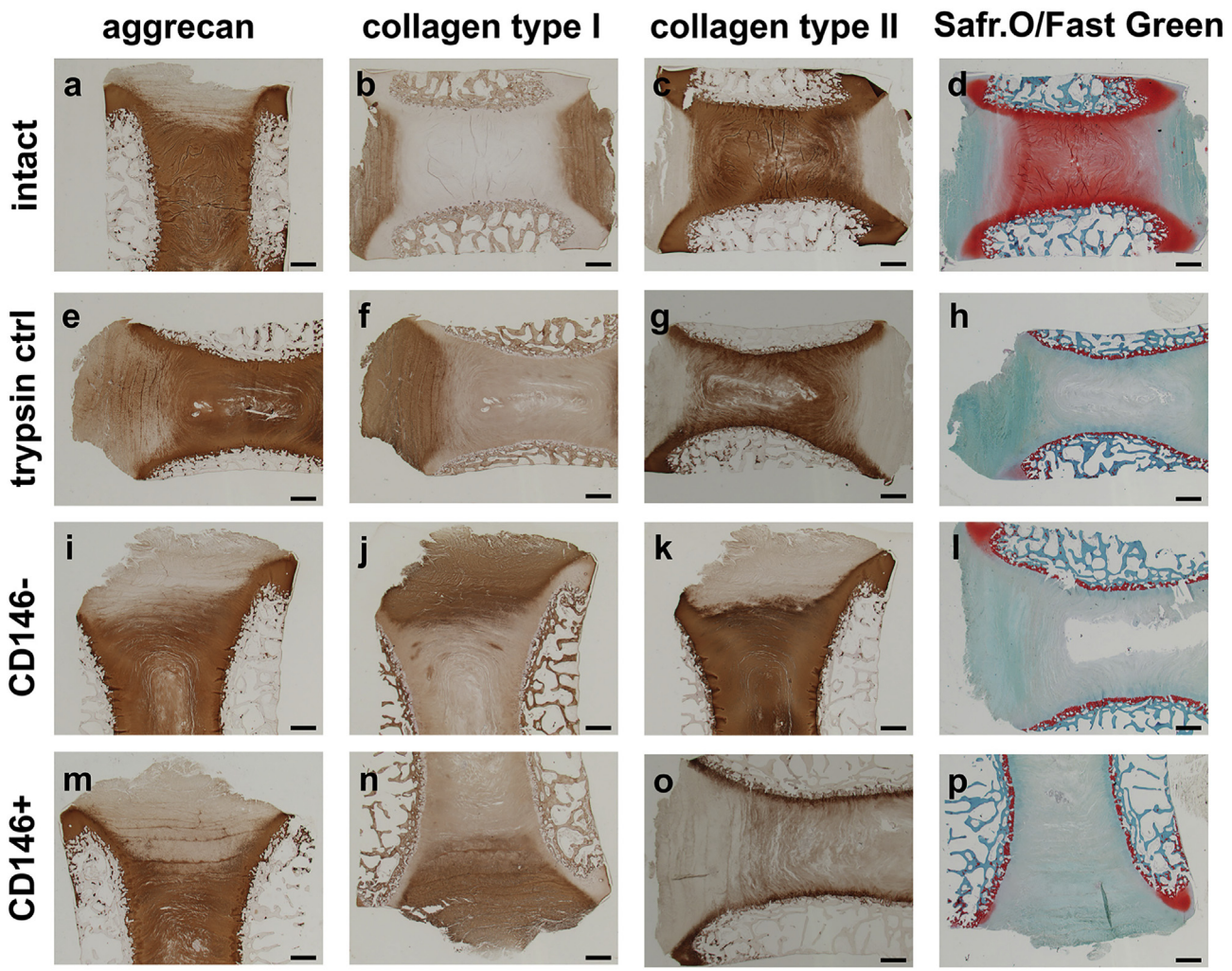

Fig. 7. Overviews of the trypsin-induced degenerated IVDs following treatment by MSC injection. Immunohistochemical staining for aggrecan, collagen type I and type II, and Safranin O/Fast Green staining were performed on intact discs (**a-d**), trypsin-injected (trypsin ctrl) (**e-h**), discs treated with CD146- MSCs (CD146-) (**i-l**) and discs treated with CD146+ MSCs (CD146+) (**m-p**). The selected images were taken from discs treated with MSCs from the same donor and bovine tail to allow a direct comparison among groups. Note that the orientation of the sections varies to allow the best visualization of the endplates and the disc annulus and nucleus regions. Scale bar equals 1 mm.

To characterize the migrating MSC subpopulation's gene expression profile, an *in vitro* migration assay towards CCL5, the main chemoattractant released by induced-degenerated IVDs, was performed[21]. Most of the surface markers analyzed (Table I) were more highly expressed in migrated compared to non-migrated cells (e.g., chemotaxis or αMEM control group, Fig. 1), suggesting that the migration process itself might influence the MSC phenotype. The concept of mechanotransduction (i.e., translation of mechanical stimuli to intracellular signals) has been described in various tissue types[39]. Specifically, actin cytoskeleton rearrangement during cell migration is considered an important regulative factor, influencing MSC phenotype by mechanical activation[40–42]. Therefore, the migration process may activate MSCs, allowing them to quickly adapt as they migrate towards the injury site. However, further investigation is required to determine whether MSCs up-regulate the analyzed markers during migration or the migrating subpopulation already expresses them in higher amounts.

CD146 expression has been connected to different biological functions, involving cell migration, proliferation, and differentiation[25,43–48]. We found that CD146 expression was associated with enhanced migration both *in vitro* and in organ culture (Figs. 2 and 3), in agreement with findings by Harkness *et al.*, who reported a higher migration of CD146+ MSCs following intravenous injection in an immuno-deficient mouse closed femoral fracture model compared to CD146- cells[27]. The higher migration capacity of CD146+ MSCs has been related to Wnt5a mediated activation of c-jun amino-terminal kinase (JNK) leading to increased cell protrusion[43].

Two different mechanisms of action have been described for MSCs' regenerative role in damaged tissues. Firstly, MSCs can differentiate into specific phenotypes and produce new ECM. Secondly, cytokines from damaged tissues can induce MSCs to release trophic factors that foster the endogenous cell population's regenerative capacity. Hence, we analyzed both the differentiation potential and paracrine effect of CD146+ and CD146- cells on induced-degenerative IVDs.

To characterize the discogenic differentiation potential of CD146+ and CD146- subpopulations, we performed GDF6-supplemented *in vitro* pellet culture[28]. While CD146- MSCs maintained a low CD146 expression, CD146+ MSCs lost CD146 expression over time, suggesting that the more progenitor-like CD146+ cell population loses this marker as it differentiates toward a more mature cell phenotype (Fig. 4b)[27]. CD146+ pellets produced significantly higher amounts of sGAG/DNA, confirming their higher NP cell-like differentiation potential in response to

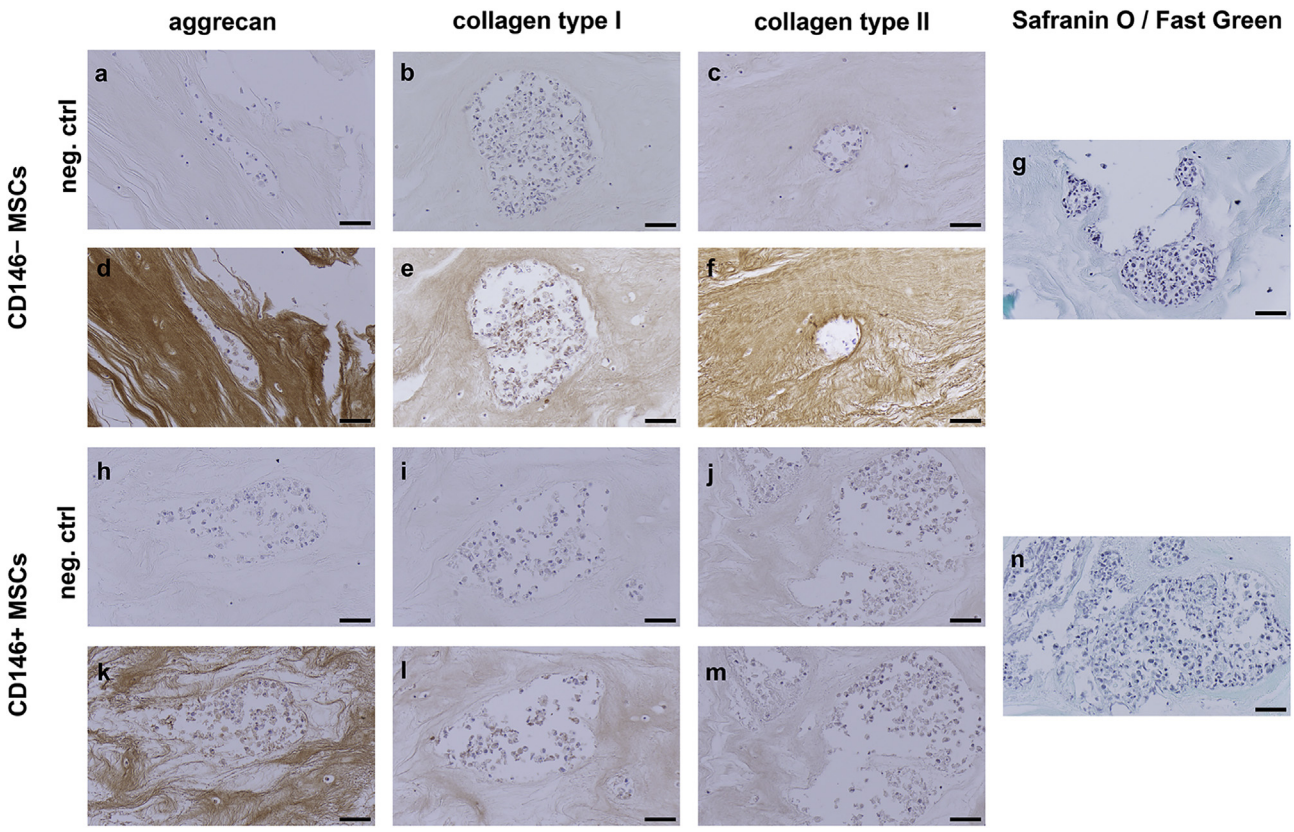

Fig. 8. Detailed view of the region where MSCs were injected in trypsin-induced degenerated IVDs. Immunohistochemical staining for aggrecan, collagen type I and type II, and Safranin O/Fast Green staining of discs treated with CD146- MSCs (**a-g**) and discs treated with CD146+ MSCs (**h-n**). Note the stronger coloration of the IVD tissue for aggrecan and type II collagen following treatment with CD146- MSCs compared to CD146+ MSCs. Scale bar equals 50 μm.

GDF6 (Fig. 4e). Based on the work of Ye *et al.*, CD146 negatively regulates canonical Wnt signaling at the β-catenin level and acts as Wnt5a receptor in the regulation of non-canonical Wnt signaling[43]. As reviewed by Ma *et al.*[49] and Usami *et al.*[50], increase in Wnt5 expression and decrease in β-catenin are distinctive features of early-stage chondrogenesis. Hence, we hypothesize that the higher GAG/DNA ratio observed in CD146+ vs CD146- MSC pellets could be due to their commitment toward the chondrogenic phenotype resulting from the activation of the Wnt5 non-canonical signaling and inhibition of canonical Wnt signaling at the β-catenin level.

While Col1 was present in both pellets at the protein level (Fig. 5), the Runx2/Sox9 ratio of the CD146- (0.95 ± 0.22) and CD146+ (0.75 ± 0.18) was lower than the critical value of 2 (predictive of osteogenic differentiation)[51]. The measured stiffness (64.3 and 45.6 kPa for CD146-and CD146+ pellets, respectively) lied within the range of human NP (~6 kPa) and AF tissue (~110 kPa)[52].

To investigate the regenerative capacity of CD146+ and CD146- MSCs in organ culture, we treated degenerated IVDs with either MSC injection or homing (Fig. 6)[31]. For both strategies, sGAG synthesis rate and staining intensity for aggrecan were higher in CD146- treated IVDs, suggesting that these more mature cells release a secretome conducive to higher regeneration of damaged tissue. Overall, CD146- MSCs were more effective in promoting an anabolic response in trypsin-induced degenerated and ECM-depleted IVDs.

Limitations

This study solely investigated the regenerative potential of bone-marrow derived MSCs, which can be obtained autologously during fusion surgery, or from an allogeneic source. IVD progenitor/stem cells from the CEP[53] or niche areas within the IVD represent alternative allogeneic sources[54]. Further investigations are needed to compare the potential of bone-marrow derived MSCs vs IVD progenitor cells. Since most MSC donors used in this study were male trauma patients there might be a selection bias. However, no differences were observed between female and male, or younger and older donors (Suppl. Figs. 2b and c). A single marker characterization was used to increase the translatability toward a clinical application; nonetheless, multiple markers might reveal an even more potent (although smaller in number) subpopulation. The bovine degenerated IVD organ culture model does not fully recapitulate the human disease but enables the establishment of a proof-of-concept of a potential clinical treatment. Notably, given the limited number of MSC donors investigated, the experiments presented in this work should be viewed as exploratory and hypothesis-generating.

Conclusions and perspectives

Our data indicate for the first time that CD146 distinguishes stem cell subpopulations with distinct migration and regenerative potential in degenerative IVDs. *In vitro* and organ culture experiments characterized a CD146+ MSC subpopulation with higher migration potential toward degenerative IVDs. The CD146+ subpopulation *in vitro* showed a superior disc-like differentiation, while the CD146- subpopulation induced a stronger regenerative response in organ culture, highlighting the importance of testing regenerative treatments in advanced whole tissue culture models of damaged

tissues. In our future work, we intend to confirm our findings *in vivo* using an adapted transpedicular approach for MSC delivery[55].

With respect to clinical translation, IVDs adjacent to a fused segment and IVDs with an AF defect represent potential clinical targets. Unlike MSC injection, homing from the endplate into the IVD avoids iatrogenic AF damage, which potentially leads to degeneration[16]. Independent of the application route (injection vs migration), our results indicate that CD146- MSCs induce a higher regenerative response, possibly due to a more differentiated state. Thereby, CD146+ MSCs would be applied for cell re-population, while CD146- cells would be preferred for stimulation of endogenous IVD cells. Importantly, given the limited number of donors used in this study, further investigations are required to assess the feasibility of this approach from a clinical translation perspective.

Author contributions

S. Wangler, U. Menzel, Z. Li, J. Ma, L.M. Benneker, S. Hoppe, M. Alini, S. Grad and M. Peroglio contributed to (1) the conception and design of the study, or acquisition of data, or analysis and interpretation of data, (2) drafting the article or revising it critically for important intellectual content and (3) final approval of the version to be submitted.

Conflict of interest

The authors declare no conflict of interest.

Acknowledgements

The authors would like to gratefully acknowledge N. Goudsouzian, D. Nehrbass and M. Bluvol for their assistance with histological preparations and R. Peter for the technical support with the bovine tails. The aggrecan and CIICI antibodies were obtained from the Developmental Studies Hybridoma Bank, created by the NICHD of the NIH and maintained at the University of Iowa, Department of Biology, Iowa City, IA, USA. The BD FACSAria III was donated by the Innovationsstiftung Graubünden. The study was funded by the AO Foundation, AOSpine International, and partially supported by a grant from the National Natural Science Foundation of China (Grant Number: 81772333).

Supplementary data

Supplementary data to this article can be found online at https://doi.org/10.1016/j.joca.2019.04.002.

References

1. Vergroesen PP, Kingma I, Emanuel KS, Hoogendoorn RJ, Welting TJ, van Royen BJ, *et al.* Mechanics and biology in intervertebral disc degeneration: a vicious circle. Osteoarthritis Cartilage 2015;23(7):1057–70.
2. Risbud MV, Shapiro IM. Role of cytokines in intervertebral disc degeneration: pain and disc content. Nat Rev Rheumatol 2014;10(1):44–56.
3. Urban JP, Roberts S. Degeneration of the intervertebral disc. Arthritis Res Ther 2003;5(3):120–30.
4. Grunhagen T, Shirazi-Adl A, Fairbank JC, Urban JP. Intervertebral disk nutrition: a review of factors influencing concentrations of nutrients and metabolites. Orthop Clin N Am 2011;42(4):465–77. vii.
5. Risbud MV, Albert TJ, Guttapalli A, Vresilovic EJ, Hillibrand AS, Vaccaro AR, *et al.* Differentiation of mesenchymal stem cells towards a nucleus pulposus-like phenotype in vitro: implications for cell-based transplantation therapy. Spine 2004;29(23):2627–32.
6. Stoyanov JV, Gantenbein-Ritter B, Bertolo A, Aebli N, Baur M, Alini M, *et al.* Role of hypoxia and growth and differentiation factor-5 on differentiation of human mesenchymal stem cells towards intervertebral nucleus pulposus-like cells. Eur Cells Mater 2011;21:533–47.
7. Dai J, Wang H, Liu G, Xu Z, Li F, Fang H. Dynamic compression and co-culture with nucleus pulposus cells promotes proliferation and differentiation of adipose-derived mesenchymal stem cells. J Biomech 2014;47(5):966–72.
8. Richardson SM, Walker RV, Parker S, Rhodes NP, Hunt JA, Freemont AJ, *et al.* Intervertebral disc cell-mediated mesenchymal stem cell differentiation. Stem Cell 2006;24(3):707–16.
9. Le Maitre CL, Baird P, Freemont AJ, Hoyland JA. An in vitro study investigating the survival and phenotype of mesenchymal stem cells following injection into nucleus pulposus tissue. Arthritis Res Ther 2009;11(1):R20.
10. Strassburg S, Richardson SM, Freemont AJ, Hoyland JA. Co-culture induces mesenchymal stem cell differentiation and modulation of the degenerate human nucleus pulposus cell phenotype. Regen Med 2010;5(5):701–11.
11. Xu Y, Zhang XJ, Fang L, Zhao TB. Co-culture of annulus fibrosus cells and bone marrow mesenchymal stem cells. Genet Mol Res 2015;14(2):3932–8.
12. Sakai D, Andersson GB. Stem cell therapy for intervertebral disc regeneration: obstacles and solutions. Nat Rev Rheumatol 2015;11(4):243–56.
13. Sakai D, Schol J. Cell therapy for intervertebral disc repair: clinical perspective. J Orthop Translat 2017;9:8–18.
14. Wuertz K, Godburn K, Iatridis JC. MSC response to pH levels found in degenerating intervertebral discs. Biochem Biophys Res Commun 2009;379(4):824–9.
15. Elabd C, Centeno CJ, Schultz JR, Lutz G, Ichim T, Silva FJ. Intradiscal injection of autologous, hypoxic cultured bone marrow-derived mesenchymal stem cells in five patients with chronic lower back pain: a long-term safety and feasibility study. J Transl Med 2016;14:253.
16. Korecki CL, Costi JJ, Iatridis JC. Needle puncture injury affects intervertebral disc mechanics and biology in an organ culture model. Spine 2008;33(3):235–41.
17. Illien-Junger S, Pattappa G, Peroglio M, Benneker LM, Stoddart MJ, Sakai D, *et al.* Homing of mesenchymal stem cells in induced degenerative intervertebral discs in a whole organ culture system. Spine 2012;37(22):1865–73.
18. Pereira CL, Teixeira GQ, Ribeiro-Machado C, Caldeira J, Costa M, Figueiredo F, *et al.* Mesenchymal stem/stromal cells seeded on cartilaginous endplates promote intervertebral disc regeneration through extracellular matrix remodeling. Sci Rep 2016;6:33836.
19. Illien-Junger S, Gantenbein-Ritter B, Grad S, Lezuo P, Ferguson SJ, Alini M, *et al.* The combined effects of limited nutrition and high-frequency loading on intervertebral discs with endplates. Spine 2010;35(19):1744–52.
20. Spaeth EL, Marini FC. Dissecting mesenchymal stem cell movement: migration assays for tracing and deducing cell migration. Methods Mol Biol 2011;750:241–59.
21. Pattappa G, Peroglio M, Sakai D, Mochida J, Benneker LM, Alini M, *et al.* CCL5/RANTES is a key chemoattractant released by degenerative intervertebral discs in organ culture. Eur Cells Mater 2014;27:124–36. discussion 36.
22. Baek SJ, Kang SK, Ra JC. In vitro migration capacity of human adipose tissue-derived mesenchymal stem cells reflects their expression of receptors for chemokines and growth factors. Exp Mol Med 2011;43(10):596–603.

23. Risbud MV, Guttapalli A, Tsai TT, Lee JY, Danielson KG, Vaccaro AR, *et al*. Evidence for skeletal progenitor cells in the degenerate human intervertebral disc. Spine 2007;32(23): 2537–44.
24. Sakai D, Nakamura Y, Nakai T, Mishima T, Kato S, Grad S, *et al*. Exhaustion of nucleus pulposus progenitor cells with ageing and degeneration of the intervertebral disc. Nat Commun 2012;3:1264.
25. Segers VF, Van Riet I, Andries LJ, Lemmens K, Demolder MJ, De Becker AJ, *et al*. Mesenchymal stem cell adhesion to cardiac microvascular endothelium: activators and mechanisms. Am J Physiol Heart Circ Physiol 2006;290(4):H1370–7.
26. Zhu H, Mitsuhashi N, Klein A, Barsky LW, Weinberg K, Barr ML, *et al*. The role of the hyaluronan receptor CD44 in mesenchymal stem cell migration in the extracellular matrix. Stem Cell 2006;24(4):928–35.
27. Harkness L, Zaher W, Ditzel N, Isa A, Kassem M. CD146/MCAM defines functionality of human bone marrow stromal stem cell populations. Stem Cell Res Ther 2016;7:4.
28. Clarke LE, McConnell JC, Sherratt MJ, Derby B, Richardson SM, Hoyland JA. Growth differentiation factor 6 and transforming growth factor-beta differentially mediate mesenchymal stem cell differentiation, composition, and micromechanical properties of nucleus pulposus constructs. Arthritis Res Ther 2014;16(2):R67.
29. Gardner OFW, Musumeci G, Neumann AJ, Eglin D, Archer CW, Alini M, *et al*. Asymmetrical seeding of MSCs into fibrin-poly(ester-urethane) scaffolds and its effect on mechanically induced chondrogenesis. J Tissue Eng Regenerat Med 2017;11(10):2912–21.
30. Oliver WC, Pharr GM. An improved technique for determining hardness and elastic modulus using load and displacement sensing indentation experiments. J Mater Res 2011;7(6): 1564–83.
31. Jim B, Steffen T, Moir J, Roughley P, Haglund L. Development of an intact intervertebral disc organ culture system in which degeneration can be induced as a prelude to studying repair potential. Eur Spine J 2011;20(8):1244–54.
32. Vadala G, Russo F, Pattappa G, Peroglio M, Stadelmann VA, Roughley P, *et al*. A nucleotomy model with intact annulus fibrosus to test intervertebral disc regeneration strategies. Tissue Eng C Methods 2015;21(11):1117–24.
33. Tischer T, Milz S, Maier M, Schieker M, Benjamin M. An immunohistochemical study of the rabbit suprapatella, a sesamoid fibrocartilage in the quadriceps tendon containing aggrecan. J Histochem Cytochem 2002;50(7):955–60.
34. Fragkakis EM, El-Jawhari JJ, Dunsmuir RA, Millner PA, Rao AS, Henshaw KT, *et al*. Vertebral body versus iliac crest bone marrow as a source of multipotential stromal cells: comparison of processing techniques, tri-lineage differentiation and application on a scaffold for spine fusion. PLoS One 2018;13(5), e0197969.
35. Tan AR, Alegre-Aguaron E, O'Connell GD, VandenBerg CD, Aaron RK, Vunjak-Novakovic G, *et al*. Passage-dependent relationship between mesenchymal stem cell mobilization and chondrogenic potential. Osteoarthritis Cartilage 2015;23(2): 319–27.
36. Yoshikawa T, Ueda Y, Miyazaki K, Koizumi M, Takakura Y. Disc regeneration therapy using marrow mesenchymal cell transplantation: a report of two case studies. Spine 2010;35(11): E475–80.
37. Orozco L, Soler R, Morera C, Alberca M, Sanchez A, Garcia-Sancho J. Intervertebral disc repair by autologous mesenchymal bone marrow cells: a pilot study. Transplantation 2011;92(7):822–8.
38. Noriega DC, Ardura F, Hernandez-Ramajo R, Martin-Ferrero MA, Sanchez-Lite I, Toribio B, *et al*. Intervertebral disc repair by allogeneic mesenchymal bone marrow cells: a randomized controlled trial. Transplantation 2017;101(8): 1945–51.
39. Martins RP, Finan JD, Guilak F, Lee DA. Mechanical regulation of nuclear structure and function. Annu Rev Biomed Eng 2012;14:431–55.
40. Rubin J, Sen B. Actin up in the nucleus: regulation of actin structures modulates mesenchymal stem cell differentiation. Trans Am Clin Climatol Assoc 2017;128:180–92.
41. Li X, He L, Yue Q, Lu J, Kang N, Xu X, *et al*. MiR-9-5p promotes MSC migration by activating beta-catenin signaling pathway. Am J Physiol Cell Physiol 2017;313(1):C80–93.
42. Uzer G, Bas G, Sen B, Xie Z, Birks S, Olcum M, *et al*. Sun-mediated mechanical LINC between nucleus and cytoskeleton regulates betacatenin nuclear access. J Biomech 2018;74:32–40.
43. Ye Z, Zhang C, Tu T, Sun M, Liu D, Lu D, *et al*. Wnt5a uses CD146 as a receptor to regulate cell motility and convergent extension. Nat Commun 2013;4:2803.
44. Wang Z, Yan X. CD146, a multi-functional molecule beyond adhesion. Cancer Lett 2013;330(2):150–62.
45. Espagnolle N, Guilloton F, Deschaseaux F, Gadelorge M, Sensebe L, Bourin P. CD146 expression on mesenchymal stem cells is associated with their vascular smooth muscle commitment. J Cell Mol Med 2014;18(1):104–14.
46. Gothard D, Greenhough J, Ralph E, Oreffo RO. Prospective isolation of human bone marrow stromal cell subsets: a comparative study between Stro-1-, CD146- and CD105-enriched populations. J Tissue Eng 2014;5. 2041731414551763.
47. Wu CC, Liu FL, Sytwu HK, Tsai CY, Chang DM. CD146+ mesenchymal stem cells display greater therapeutic potential than CD146- cells for treating collagen-induced arthritis in mice. Stem Cell Res Ther 2016;7:23.
48. Moreno-Fortuny A, Bragg L, Cossu G, Roostalu U. MCAM contributes to the establishment of cell autonomous polarity in myogenic and chondrogenic differentiation. Biol Open 2017;6(11):1592–601.
49. Ma B, Landman EB, Miclea RL, Wit JM, Robanus-Maandag EC, Post JN, *et al*. WNT signaling and cartilage: of mice and men. Calcif Tissue Int 2013;92(5):399–411.
50. Usami Y, Gunawardena AT, Iwamoto M, Enomoto-Iwamoto M. Wnt signaling in cartilage development and diseases: lessons from animal studies. Lab Invest 2016;96(2):186–96.
51. Loebel C, Czekanska EM, Bruderer M, Salzmann G, Alini M, Stoddart MJ. In vitro osteogenic potential of human mesenchymal stem cells is predicted by Runx2/Sox9 ratio. Tissue Eng 2015;21(1–2):115–23.
52. Umehara S, Tadano S, Abumi K, Katagiri K, Kaneda K, Ukai T. Effects of degeneration on the elastic modulus distribution in the lumbar intervertebral disc. Spine 1996;21(7):811–9. discussion 20.
53. Liu LT, Huang B, Li CQ, Zhuang Y, Wang J, Zhou Y. Characteristics of stem cells derived from the degenerated human intervertebral disc cartilage endplate. PLoS One 2011;6(10), e26285.
54. Henriksson H, Thornemo M, Karlsson C, Hagg O, Junevik K, Lindahl A, *et al*. Identification of cell proliferation zones, progenitor cells and a potential stem cell niche in the intervertebral disc region: a study in four species. Spine 2009;34(21): 2278–87.
55. Vadala G, Russo F, Pattappa G, Schiuma D, Peroglio M, Benneker LM, *et al*. The transpedicular approach as an alternative route for intervertebral disc regeneration. Spine 2013; 38(6):E319–24.